268, 16430 (1993); P. C. Chen, G. C. DuBois, M. Chen, *J. Biol. Chem.* **270**, 2874 (1995); T. Reid, P. Louie, R. A. Heller, *Circ. Shock* **44**, 84 (1994); A. E. Corcoran *et al.*, *Eur. J. Biochem.* **223**, 831 (1994).
15. Mutagenesis was performed with the Quikchange method (Stratagene) as per the manufacturer's instructions. The mutations were confirmed by DNA sequencing.
16. Single-letter abbreviations for the amino acid residues are as follows: A, Ala; C, Cys; D, Asp; E, Glu; F, Phe; G, Gly; H, His; I, Ile; K, Lys; L, Leu; M, Met; N, Asn; P, Pro; Q, Gln; R, Arg; S, Ser; T, Thr; V, Val; W, Trp; and Y, Tyr.
17. L. Tron *et al.*, *Biophys. J.* **45**, 939 (1984); J. Szollosi *et al.*, *Cytometry* **5**, 210 (1984).
18. R. Y. Tsien, *Annu. Rev. Biochem.* **67**, 509 (1998).
19. R. M. Siegel *et al.*, *Science* **288**, 2354 (2000); R. M. Siegel *et al.*, "Measurement of molecular interactions in living cells by fluorescence resonance energy transfer between variants of the green fluorescent protein," *Science*'s STKE (2000) (www.stke.org/cgi/content/full/OC_sigtrans;2000/38/pl1).
20. G. Papoff *et al.*, *J. Biol. Chem.* **274**, 38241 (1999).
21. J. Naismith *et al.*, *J. Biol. Chem.* **270**, 13303 (1995); J. Naismith *et al.*, *Structure* **4**, 1251 (1996); J. Naismith *et al.*, *J. Mol. Recog.* **9**, 113 (1995).
22. F. K.-M. Chan and M. J. Lenardo, *Eur. J. Immunol.* **30**, 652 (2000).
23. R. A. Heller *et al.*, *Cell* **70**, 47 (1992); T. Weiss *et al*, *J. Immunol.* **158**, 2398 (1997); V. Haridas *et al.*, *J. Immunol.* **160**, 3152 (1998); W. Declercq *et al.*, *J. Immunol.* **161**, 390 (1998).
24. C. Guo, S. K. Dower, D. Howlowka, B. Baird, *J. Biol. Chem.* **270**, 27562 (1995); S. Damjanovich *et al.*, *Proc. Natl. Acad. Sci. U.S.A.* **93**, 13973 (1996); T. Gadella Jr. and T. M. Jovin, *J. Cell. Biol.* **129**, 1543 (1995).
25. O. Livnah *et al.*, *Science* **283**, 987 (1999); I. Remy, I. A. Wilson, S. W. Michnick, *Science* **283**, 990 (1999).
26. Receptor expression was monitored by staining with monoclonal antibodies to HA and p80 (clone MAB226, R&D Systems). TNF-α binding was determined with biotinylated TNF-α (NEN Life Sciences) and a secondary fluorescein-conjugated streptavidin label. Samples were analyzed on a FACScan flow cytometer. Results shown are representative of at least five experiments.
27. Fifteen micrograms of the corresponding plasmids were transfected into p80 Jurkat cells (*22*) by electroporation using a BTX Electro Cell Manipulator 600. After 9 to 24 hours, cells were stimulated with the indicated amount of TNF-α for 12 to 16 hours. Cells were then stained for HA expression and propidium iodide uptake. The number of HA-positive cells was scored under constant time, and percent inhibition of apoptosis was calculated by normalizing to the percentage of cell death induced in the HveAΔCD-HA–transfected samples. Results are representative of three experiments.
28. We thank P. Scheurich, P. Spear, A. Winoto, and J. Woronicz for providing us with antibodies and plasmids; L. D'Adamio, R. Germain, W. Leonard, D. Levens, H. Metzger, J. O'Shea, W. Paul, and T. Waldmann for critical reading of the manuscript; K. Holmes, R. Swofford, and D. Stephany for help with the fluorescence energy transfer studies; M. Boguski for bioinformatics assistance; and the members of the Lenardo lab for discussion. F.K.-M.C. is supported by a Cancer Research Institute/Miriam and Benedict Wolf fellowship. H.J.C. is a Howard Hughes Medical Institute/National Institutes of Health research scholar.

28 December 1999; accepted 21 April 2000

Fas Preassociation Required for Apoptosis Signaling and Dominant Inhibition by Pathogenic Mutations

Richard M. Siegel,[1] John K. Frederiksen,[1] David A. Zacharias,[2] Francis Ka-Ming Chan,[1] Michele Johnson,[1] David Lynch,[3] Roger Y. Tsien,[2] Michael J. Lenardo[1]*

Heterozygous mutations encoding abnormal forms of the death receptor Fas dominantly interfere with Fas-induced lymphocyte apoptosis in human autoimmune lymphoproliferative syndrome. This effect, rather than depending on ligand-induced receptor oligomerization, was found to stem from ligand-independent interaction of wild-type and mutant Fas receptors through a specific region in the extracellular domain. Preassociated Fas complexes were found in living cells by means of fluorescence resonance energy transfer between variants of green fluorescent protein. These results show that formation of preassociated receptor complexes is necessary for Fas signaling and dominant interference in human disease.

Fas (CD95 or APO-1) is a cell surface receptor that transduces apoptotic signals critical for immune homeostasis and tolerance (*1–3*). The Fas protein is a 317–amino acid type 1 transmembrane glycoprotein with three extracellular cysteine-rich domains (CRDs) that are characteristic of the tumor necrosis factor receptor (TNFR) superfamily. Both Fas and Fas ligand (FasL) are predicted to form trimers, with CRD2 and CRD3 forming the major contact surfaces for FasL (*4, 5*). The Fas cytoplasmic portion contains a death domain that rapidly recruits the adaptor molecule FADD (Fas-associated death domain protein) and the caspase-8 proenzyme after binding of FasL or agonistic antibodies, leading to caspase activation and apoptosis (*6–10*).

Patients with autoimmune lymphoproliferative syndrome (ALPS) type 1A have heterozygous germ line mutations in the *APT-1* Fas gene. Their lymphocytes are resistant to Fas-induced apoptosis, and transfection of the mutant allele causes dominant interference with apoptosis induced through Fas (*11–16*). This was thought to result from ligand-mediated crosslinking of wild-type and defective Fas chains into mixed trimer complexes. However, a mutation that causes an extracellular domain deletion of most of CRD2 (ALPS Pt 2, deletion of amino acids 52 to 96) as a result of altered RNA splicing shows no binding to agonistic antibodies or FasL, but still dominantly interferes with Fas-induced apoptosis almost as efficiently as does a death domain mutant [ALPS Pt 6, $Ala^{241} \rightarrow$ Asp (A241D)] (Fig. 1A) (*13, 17*). Control experiments showed equal cell surface expression of the wild-type and mutant Fas molecules (*18*). Thus, dominant interference cannot be explained by the conventional model of signaling by FasL-induced oligomerization of receptor monomers because, in this scheme, the Pt 2 mutant Fas molecule would not become part of a mixed receptor complex. We therefore tested for ligand-independent interactions between Pt 2 Fas and wild-type Fas. Both full-length and Pt 2 Fas coprecipitated with a Fas 1–210:GFP chimera in which green fluorescent protein (GFP) replaces the death domain (Fig. 1C). This interaction was specific, because the TNFR family receptors TNFR2/p80 and HveA did not interact with Fas (*1*).

We have found that TNFR superfamily members share a self-association domain in CRD1, termed the "pre-ligand assembly domain" (PLAD) (Fig. 1B) (*19*). To test whether Fas contains a functional PLAD, we constructed hemagglutinin (HA)-tagged NH_2-terminal Fas truncations (*20*). Deleting the first subdomain in CRD1 (amino acids 1 to 42) (*21*) substantially reduced ligand binding but did not prevent binding of the Fas monoclonal antibody (mAb) APO-1. Deleting the entire CRD1 (amino acids 1 to 66) abrogated binding of both FasL and Fas mAb (Fig. 1A). Both truncations eliminated coprecipitation with a differentially tagged Fas molecule and abrogated apoptosis signaling; this result indicates that the NH_2-terminus of Fas, including CRD1, functions as a PLAD (Fig. 1, C

[1]Laboratory of Immunology, National Institute of Allergy and Infectious Diseases, National Institutes of Health, Bethesda, MD 20892, USA. [2]Howard Hughes Medical Institute and Department of Pharmacology, University of California, San Diego School of Medicine, La Jolla, CA 92093, USA. [3]Immunex Corporation, 51 University Street, Seattle, WA 98101, USA.

*To whom correspondence should be addressed. E-mail: lenardo@nih.gov

and D) (*19, 22*). Fas mutants from ALPS patients with truncated or mutated death domains are potent dominant-negative inhibitors of normal Fas function. However, if the PLAD was removed from Fas molecules lacking the death domain (Fas 1–210) or harboring an ALPS death domain point mutation [ALPS Pt 26, $Asp^{244} \rightarrow Val$ (D244V)], dominant interference was lost (Fig. 1D).

To further explore the requirement for ligand binding in receptor self-association, we tested the Fas point mutation $Arg^{86} \rightarrow Ser$ (R86S) that removes a critical CRD2 contact residue for FasL (*5*) and prevents FasL binding (Fig. 1A). The overall receptor structure was preserved, as indicated by staining with APO-1 and DX2 Fas mAbs (Fig. 1A) (*18*), and self-association with wild-type Fas still occurred (Fig. 1C). Even though it could not bind FasL, this mutant dominantly interfered with FasL-induced apoptosis through wild-type Fas (Fig. 1E). Apoptosis induced by Fas mAb in the same cells was unimpaired, which indicated that Fas was functionally expressed on the cell surface (Fig. 1E). Thus, receptor self-association is independent of ligand binding, yet critical for both normal function and dominant interference.

To quantitate Fas receptor self-association in living cells, we developed flow cytometric and microscopic assays based on fluorescence resonance energy transfer (FRET) between spectral variants of GFP. [See protocol at *Science*'s STKE (www.stke.org/cgi/content/full/OC_sigtrans;2000/38/pl1)]. When in close proximity (<100 Å), cyan fluorescent protein (CFP) and yellow fluorescent protein (YFP) will exhibit FRET (*23*). Flow cytometry using CFP excitation of cells expressing both CFP and YFP Fas fusion proteins triggered strong fluorescence emission at the YFP wavelength attributable to FRET (Fig. 2A) (*24*). FRET was detected between Fas fusion proteins with or without the death domain, but not between Fas and other TNFR family members, such as TNFR1/p60, HveA, or DR4 (Fig. 2) (*1, 18*). Microscopic measurement of CFP dequenching after selectively photobleaching YFP yielded a FRET efficiency of 11%. With the death domain on both molecules, FRET efficiency rose to 23%, consistent with increased oligomerization via the death domain (*25*). Pt 2 Fas gave a FRET efficiency comparable to that of Fas 1–210, but there was reduced signal with Fas 43–210 and no detectable FRET with Fas 67–210 or the DR4 control (Fig. 2B). Hence, Fas molecules are in close proximity on the surface of living cells, and this proximity depends on the PLAD.

To test whether native Fas receptors normally self-associate, we performed chemical crosslinking studies on H9 T lymphoma cells expressing endogenous human Fas (Fig. 3). Crosslinking shifted the apparent molecular size of Fas in deglycosylated cell lysates from 45 to 140 kD under nonreducing conditions (Fig. 3A). Densitometry suggested that 60% of the Fas chains were crosslinked. Unlike FasL- or Fas mAb–treated cells, Fas complexes from surface-crosslinked cells showed only partial recruitment of FADD and no recruitment of caspase-8, with no cleavage of the downstream caspase substrate poly-(ADP-ribose)polymerase (PARP). Interestingly, crosslinking prevented the formation of active signaling complexes in response to subsequent treatment with agonistic mAb (Fig. 3B).

Our findings redefine how death signals

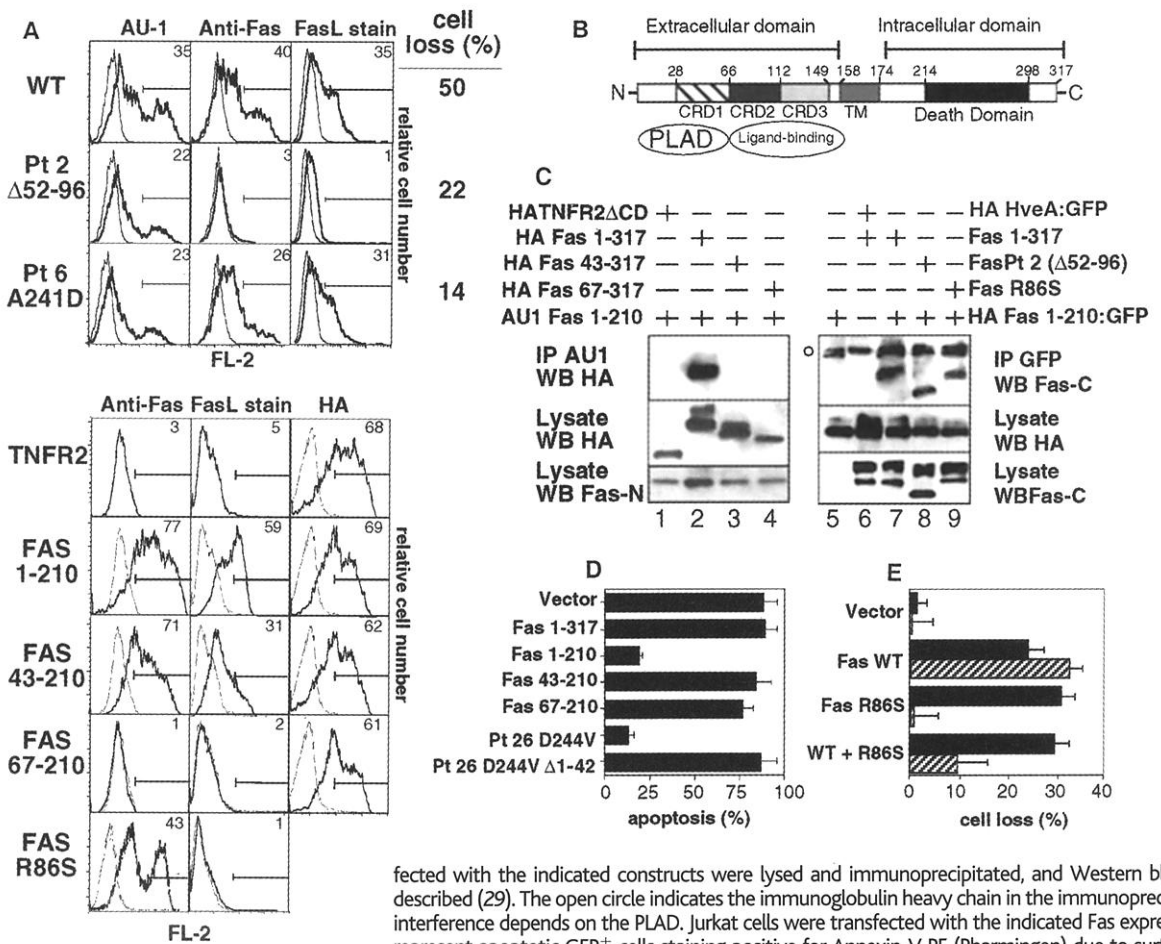

Fig. 1. (**A**) Surface expression and binding characteristics of the indicated wild-type and mutant Fas molecules transfected into 293T HEK cells. The bold line shows specific staining and the thin line indicates background staining of mock-transfected cells. AU-1 or HA staining was performed to confirm surface expression of each protein. Staining of functional receptors with FasL was performed with a preparation of FasL trimerized via a modified leucine zipper (FasL-LZ) and LZ mAb. Numbers indicate the percentage of positively staining cells in the indicated gates. Cell loss of transfected murine BW cells was calculated as described (*13, 22*). (**B**) Schematic of the Fas protein. Numbering is based on (*21*). TM, transmembrane domain. (**C**) Self-association of Fas molecules. 293T cells cotransfected with the indicated constructs were lysed and immunoprecipitated, and Western blots (WB) were probed as described (*29*). The open circle indicates the immunoglobulin heavy chain in the immunoprecipitates (IP). (**D**) Dominant interference depends on the PLAD. Jurkat cells were transfected with the indicated Fas expression vectors. Percentages represent apoptotic GFP^+ cells staining positive for Annexin-V PE (Pharmingen) due to surface exposure of phosphatidylserine after treatment with Fas mAb (*15*). Results are representative of three independent transfections. (**E**) Induction and inhibition of apoptosis by the non–ligand-binding R86S Fas mutant. Murine BW cells were transfected with the indicated expression vectors, and apoptosis was induced with Fas mAb (solid bars) and FasL (hatched bars) as described (*13, 22*).

are triggered through Fas and how mutations in ALPS dominantly interfere with normal Fas function. In a large number of ALPS patients evaluated at the National Institutes of Health (*13–15, 17*), we found that the PLAD was preserved in every example of a dominant-interfering mutation associated with disease, including mutations that create premature termination polypeptides encoding only the first 57 and 62 amino acids of the mature Fas protein. To cause dominant interference, mutant proteins must physically interact with wild-type proteins in a functional complex (*26*). Previously, dominant-negative receptor mutations associated with human diseases have been shown to interfere with normal receptor signaling by sequestering ligand, blocking intracellular signaling, or preventing transport of the wild-type chain to the cell surface (*27*). For Fas, dominant interference stems instead from PLAD-mediated association between wild-type and mutant receptors before ligand binding. PLAD interactions are essential for ligand binding and signaling and have been observed in the regulation of apoptosis by soluble alternatively spliced forms of Fas that all include this domain (*28*). PLAD-mediated dominant interference may also play a role in modulation of signaling by decoy receptors (*2*) and in the pathogenesis of diseases due to heterozygous genetic abnormalities in other members of the TNFR superfamily.

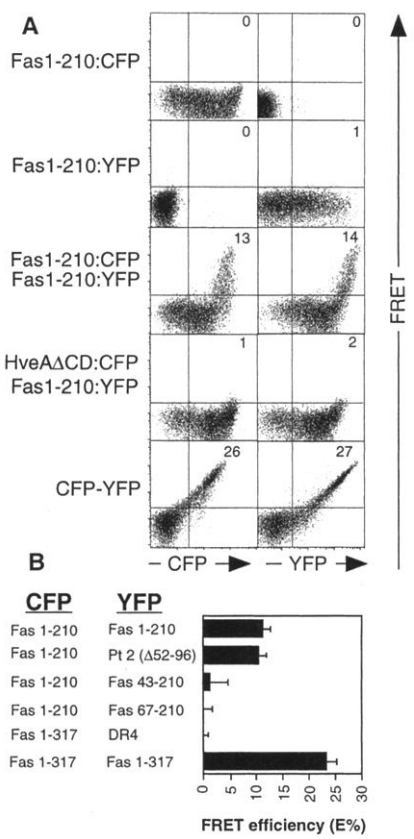

Fig. 2. (**A**) Dot plots showing relationships between CFP, YFP, and FRET signals in the indicated cotransfectants. CFP and YFP fusion proteins were constructed, transfected into 293T cells, and analyzed on a FACSvantage cytometer (*24*). Numbers are the percentage of cells positive for CFP or YFP with FRET signal (top right quadrant). The bottom panel shows FRET from a construct in which CFP was covalently fused to YFP through a nine–amino acid peptide linker (CFP-YFP) (*30*). (**B**) FRET efficiency (E%) for the indicated CFP and YFP pairs, as determined by CFP dequenching after photobleaching of YFP on individual cells (five readings of four- to seven-cell regions) (*24*). The numbers represent the average E% and standard error for each plasmid pair.

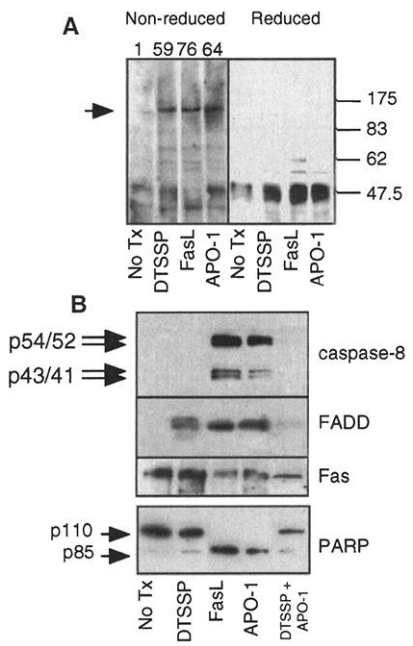

Fig. 3. Preassociation of endogenous Fas receptor chains. H9 lymphoma cells (10^7) were treated for 30 min with 10 mM of the thiol-cleavable crosslinker 3,3′-dithiobis[sulfosuccinimidyl propionate] (DTSSP) and/or stimulated with the indicated reagents or were incubated in medium alone (No Tx). (**A**) Western blots of deglycosylated cell lysates run under reducing or nonreducing conditions were treated with and probed with Fas mAb. The arrow indicates the position of the major crosslinked species. Size markers (in kilodaltons) are at the right. (**B**) After treatment with the indicated reagents, cells were lysed, immunoprecipitated, and blotted for FADD and caspase-8 as described (*15*). The positions of the two isoforms of procaspase-8 (p54/52) and caspase-8 cleavage products after proteolysis of the p11 caspase subunit (p43/41) are shown with arrows. PARP cleavage was analyzed on lysates from cells cultured at 37°C for an additional 4 hours after the indicated treatments. The upper band is the 115-kD full-length PARP; the lower band is the 85-kD signature fragment produced by caspase cleavage during apoptosis. The results are representative of at least three independent experiments.

References and Notes

1. D. Wallach *et al.*, *Annu. Rev. Immunol.* **17**, 331 (1999).
2. A. Ashkenazi and V. M. Dixit, *Science* **281**, 1305 (1998).
3. M. Lenardo *et al.*, *Annu. Rev. Immunol.* **17**, 221 (1999).
4. J. R. Orlinick, A. Vaishnaw, K. B. Elkon, M. V. Chao, *J. Biol. Chem.* **272**, 28889 (1997).
5. G. C. Starling *et al.*, *J. Exp. Med.* **185**, 1487 (1997).
6. A. M. Chinnaiyan, K. O'Rourke, M. Tewari, V. M. Dixit, *Cell* **81**, 505 (1995).
7. F. C. Kischkel *et al.*, *EMBO J.* **14**, 5579 (1995).
8. B. Huang, M. Eberstadt, E. T. Olejniczak, R. P. Meadows, S. W. Fesik, *Nature* **384**, 638 (1996).
9. D. A. Martin, R. M. Siegel, L. Zheng, M. J. Lenardo, *J. Biol. Chem.* **273**, 4345 (1998).
10. D. Nicholson and N. Thornberry, *Trends Biochem. Sci.* **22**, 299 (1997).
11. F. Rieux-Laucat *et al.*, *Science* **268**, 1347 (1995).
12. J. Drappa, A. K. Vaishnaw, K. E. Sullivan, J. L. Chu, K. B. Elkon, *N. Engl. J. Med.* **335**, 1643 (1996).
13. G. H. Fisher *et al.*, *Cell* **81**, 935 (1995).
14. S. E. Straus, M. Sneller, M. J. Lenardo, J. M. Puck, W. Strober, *Ann. Intern. Med.* **130**, 591 (1999).
15. D. A. Martin *et al.*, *Proc. Natl. Acad. Sci. U.S.A.* **96**, 4552 (1999).
16. A. K. Vaishnaw *et al.*, *J. Clin. Invest.* **103**, 355 (1999).
17. C. Jackson *et al.*, *Am. J. Hum. Genet.* **64**, 1002 (1998).
18. R. M. Siegel and M. J. Lenardo, unpublished data.
19. F. K.-M. Chan *et al.*, *Science* **288**, 2351 (2000).
20. Fas truncation mutants were created by polymerase chain reaction (PCR) mutagenesis with appropriate primers and Pwo high-fidelity polymerase (Roche Molecular Biochemicals). For the AU-1–tagged receptors, a template with DNA coding for the DTYRYI AU-1 epitope tag sequence previously inserted into the region upstream of Fas CRD1 was used. For HA tagging, mutations were cloned into the Eco RI–Xho I sites of a modified pCDNA3 vector containing the leader sequence of p60 followed by sequences coding for the YPYDVPDYA HA epitope tag. Point mutations were created with the Quickchange technique (Stratagene), substituting Pwo for Pfu polymerase. Mutations were verified by restriction enzyme mapping and automated sequencing.
21. J. H. Naismith and S. R. Sprang, *Trends Biochem. Sci.* **23**, 74 (1998).
22. Murine BW thymoma cell were transfected by electroporation with 10 μg of the indicated plasmids and 5 μg of the GFP reporter plasmid. After 18 hours, apoptosis was induced with Fas mAb APO-1 (500 ng/ml) or 5% v/v supernatant containing soluble FasL/leucine zipper fusion protein. Viable cell loss was quantitated as described (*13*). Cell loss induced by APO-1 for singly transfected receptors was 29% for full-length Fas (1–317), 2.9% for Fas 43–317, –1.7% for Fas 67–317, and –8.1% for vector-transfected controls.
23. A. Miyawaki and R. Y. Tsien, *Methods Enzymol.*, in press; L. Stryer, *Annu. Rev. Biochem.* **47**, 819 (1978); R. M. Siegel *et al.*, "Measurement of molecular interactions in living cells by fluorescence resonance energy transfer between variants of the green fluorescent protein," *Science*'s STKE (2000) (www.stke.org/cgi/content/full/OC_sigtrans;2000/38/pl1).
24. Fas receptors with COOH-terminal in-frame fusions to CFP and YFP (at position 210 in place of the death domain) were cotransfected into 293T HEK cells, and they were appropriately expressed on the cell surface (*18*). In-frame CFP and YFP fusions with Fas and other TNF family receptors were generated by standard PCR cloning techniques; correct protein expression was confirmed by Western blotting and fluorescence microscopy. 293T cells were transfected with 1 μg of the indicated YFP fusion protein constructs and 2 μg of the indicated CFP constructs. After 24 to 36 hours, cells were harvested in phosphate-buffered saline and analyzed on a FACSvantage cytometer (Becton Dickinson) with a krypton laser tuned to 413 nm for CFP and an air-cooled laser tuned to 514 nm for YFP. CFP was detected with a 470 nm/20 nm bandpass filter. YFP and FRET were detected with 546 nm/10 nm bandpass filters with signals from the 514- and

413-nm lasers, respectively. Cells were sequentially illuminated with the 514- and 413-nm lasers so that all three signals could be detected from each cell. Compensation was applied so that there was no FRET signal visible from cells transfected with CFP or YFP alone. We collected 50,000 events from each sample and analyzed the data with the FlowJo software package (Treestar Inc.). Another characteristic of FRET is the dequenching of donor fluorescence after photobleaching of the acceptor. This dequenching can be converted to a measurement of FRET efficiency (E%), which is related to the distance between two molecules by the Förster equation [see (*23*)]. For FRET efficiency measurements, CFP emission intensities from cotransfected cells were measured on a fluorescence microscope before and after bleaching the YFP with 5 min of illumination through a 505- to 545-nm bandpass filter. We corrected for direct bleaching of cells transfected with the CFP fusion partner alone. FRET efficiencies were calculated using the formula E% = [1 − (CFP emission before YFP bleach/CFP emission after YFP bleach)] × 100%.

25. M. P. Boldin *et al.*, *J. Biol. Chem.* **270**, 387 (1995).
26. I. Herskowitz, *Nature* **329**, 219 (1987).
27. M. P. Cosma, M. Cardone, F. Carlomagno, V. Colantuoni, *Mol. Cell. Biol.* **18**, 3321 (1998); E. Jouanguy *et al.*, *Nature Genet.* **21**, 370 (1999); R. Levy-Toledano, L. H. Caro, D. Accili, S. I. Taylor, *EMBO J.* **13**, 835 (1994).
28. G. Papoff *et al.*, *J. Biol. Chem.* **274**, 38241 (1999); G. Papoff *et al.*, *J. Immunol.* **156**, 4622 (1996).
29. 293T cells were transfected with Fugene 6 (Boehringer Mannheim) according to the manufacturer's instructions. Cells were lysed in 150 mM NaCl, 20 mM tris-Cl (pH 7.5), 1 mM EDTA, 5 mM iodoacetamide, 2 mM dithiothreitol, 10% glycerol, 1% Triton X-100, and protease inhibitors (Boehringer Mannheim). After preclearing with protein G–agarose beads (Boehringer Mannheim) and normal mouse immunoglobulin G, proteins were immunoprecipitated with 1 mg anti-GFP (Roche Molecular Biochemicals) and protein G–agarose beads. Immune complexes were washed three times with lysis buffer. AU-1 was immunoprecipitated with 2 μl of anti–AU-1 (Covance) and protein A beads. Proteins were electrophoresed on Tris/Glycine gels (Novex), transferred to nitrocellulose membranes, and blotted with the indicated antibodies. Bands were visualized with SuperSignal WestDura (Pierce). Densitometry was performed with one-dimensional image analysis software (Kodak).
30. N. P. Mahajan, D. C. Harrison-Shostak, J. Michaux, B. Herman, *Chem. Biol.* **6**, 401 (1999).
31. We thank D. Martin, L. Zheng, and D. Smith for plasmid construction; K. Holmes, R. Swofford, and D. Stephany for excellent technical assistance; M. Peter and B. Herman for valuable reagents; T. Waldmann, R. Germain, H. Metzger, J. O'Shea, C. Jackson, and F. Hornung for critical reading of the manuscript and helpful comments; and S. Starnes for editorial assistance. S. Straus, J. Puck, C. Jackson, and J. Dale of the NIH ALPS working group provided clinical material and encouragement that were essential for this work. Supported by a Cancer Research Institute/Miriam and Benedict Wolf fellowship (F.K.-M.C.), NIH grant NS27177 (R.Y.T.), and a fellowship in the HHMI/NIH scholar program (M.J.).

28 December 1999; accepted 21 April 2000

Cross Talk Between Interferon-γ and -α/β Signaling Components in Caveolar Membrane Domains

Akinori Takaoka,[1] Yukiko Mitani,[1] Hirofumi Suemori,[2] Mitsuharu Sato,[1] Taeko Yokochi,[1] Shigeru Noguchi,[2] Nobuyuki Tanaka,[1] Tadatsugu Taniguchi[1]*

Definition of cellular responses to cytokines often involves cross-communication through their respective receptors. Here, signaling by interferon-γ (IFN-γ) is shown to depend on the IFN-α/β receptor components. Although these IFNs transmit signals through distinct receptor complexes, the IFN-α/β receptor component, IFNAR1, facilitates efficient assembly of IFN-γ–activated transcription factors. This cross talk is contingent on a constitutive subthreshold IFN-α/β signaling and the association between the two nonligand-binding receptor components, IFNAR1 and IFNGR2, in the caveolar membrane domains. This aspect of signaling cross talk by IFNs may apply to other cytokines.

The cytokines IFN-α/β and IFN-γ play central roles in the innate immune response against viral infections (*1–4*). IFN-γ is also widely involved in the regulation of adaptive immune responses (*5*). These cytokines transmit signals to the cell interior through distinct receptor complexes, the IFN-α/β receptor (IFNAR) and the IFN-γ receptor (IFNGR), each composed of two type II membrane glycoproteins: IFNAR1 and IFNAR2, and IFNGR1 and IFNGR2 (*2–4*, *6–8*). Ligand-induced stimulation of each IFN receptor complex results in the activation of the receptor-associated Janus protein tyrosine kinases (Jak PTKs), specifically, Jak1 and Tyk2 PTKs for IFNAR and Jak1 and Jak2 PTKs for IFNGR (*6–10*). After activation of these Jak PTKs, the signal transducers and activators of transcription 1 (Stat1) and Stat2 are tyrosine-phosphorylated, leading to formation of the two transcriptional activators, IFN-γ–activated factor (GAF)/IFN-α–activated factor (AAF) and IFN-stimulated gene factor 3 (ISGF3)/Stat1-p48 (*9*, *11*). Although IFN-α/β and IFN-γ elicit cellular antiviral activities, it is unknown whether IFNAR and IFNGR share any functional aspects in the signaling processes. Receptors for these IFNs and other cytokines are expressed at low levels, ranging from 10^2 to 10^3 molecules on the cell surface (*2*), but can efficiently transmit signals to the cell interior. This raises the possibility that these receptors are clustered, even before ligand stimulation, to a particular region of the cell membrane.

Mouse embryonic fibroblasts (MEFs), isolated from either IFNAR1-deficient or IFNGR1-deficient mice (*12*, *13*), were examined for their antiviral response induced by IFN-γ or IFN-α (*14*). In MEFs lacking IFNAR1 (IFNAR1-null MEFs) (*15*), the IFN-γ–induced antiviral response was impaired; a concentration of IFN-γ that was 10 times higher than that for wild-type (WT) MEFs was required to achieve 50% protection of the cells from encephalomyocarditis virus (EMCV) infection, and full IFN-γ response was not achieved at even higher ligand concentrations (Fig. 1A). In contrast, the IFN-α–induced antiviral response was normal in MEFs deficient in IFN-γ receptor (IFNGR1-null MEFs). The IFN-γ–induced DNA-binding activity of Stat1 was six to seven times lower in IFNAR1-null MEFs than in WT MEFs (Fig. 1B) (*12*), although the kinetics of the Stat1 activation was the same (*16*). Similar results were obtained in splenocytes of these mutant mice (*16*), indicating that the observed defect in Stat1 activation is not restricted to MEFs. In contrast, Stat1 activation by IFN-α was normal in IFNGR1-null MEFs (*16*), consistent with the antiviral assay result. Like IFN-α/β stimulation, IFN-γ stimulation activates ISGF3 in MEFs (*17*), which is critical for the IFN-γ–induced antiviral response (*17*, *18*). In IFNAR1-null MEFs, however, IFN-γ–induced formation of the ISGF3 complex was not detected (Fig. 1B).

To determine the role of IFNAR1 in IFN-γ signaling, we expressed mutant forms of IFNAR1 (Fig. 1C) in the IFNAR1-null MEFs. Expression of WT IFNAR1 restored the IFN-γ–induced activation of Stat1 and ISGF3 (Fig. 1C, lower panel), as well as antiviral responses (Fig. 1D). However, expression of either a mutant IFNAR1 lacking the cytoplasmic region or a chimeric receptor composed of the IFNAR1 transmembrane and cytoplasmic region failed to restore the response to IFN-γ (Fig. 1, C and D).

These results raised the question of whether an intact IFNAR1 or an IFN-α/β signaling event, mediated by IFNAR1, is required to produce a complete IFN-γ response. Because low levels of IFN-α/β mRNA expression were detected by reverse

[1]Department of Immunology, Graduate School of Medicine and Faculty of Medicine, University of Tokyo, Hongo 7-3-1, Bunkyo-ku, Tokyo 113-0033, Japan. [2]Meiji Institute of Health Science, Meiji Milk Products, Naruda 540, Odawara-shi, Kanagawa 250-0862, Japan.

*To whom correspondence should be addressed. E-mail: tada@m.u-tokyo.ac.jp